A Comparative Study of Fabrication and Performance of Ni/3 mol % Y_2O_3 ZrO_2 and Ni/8 mol % Y_2O_3 ZrO_2 Cermet Electrodes

Journal of The Electrochemical Society, **150** (11) E548-E559 (2003)
0013-4651/2003/150(11)/E548/12/$7.00 © The Electrochemical Society, Inc.

A Comparative Study of Fabrication and Performance of Ni/3 mol % Y_2O_3-ZrO_2 and Ni/8 mol % Y_2O_3-ZrO_2 Cermet Electrodes

San Ping Jiang[z]

Fuel Cells Strategic Research Program, School of Manufacture and Production Engineering, Nanyang Technological University, Singapore 639798

A comparative study was carried out on the fabrication and performance of Ni/3 mol % Y_2O_3-ZrO_2 (Ni/TZ3Y) and Ni/8 mol % Y_2O_3-ZrO_2 (Ni/TZ8Y) cermet anodes. The electrochemical performance of Ni/TZ3Y and Ni/TZ8Y cermet anodes was investigated in relation to the fabrication processes such as the coarsening treatment of zirconia and Ni/zirconia cermet powder and the sintering temperature of the anode. For Ni/TZ3Y cermet electrodes, the effect of the coarsening treatment of TZ3Y and Ni/TZ3Y cermet powders on the polarization performance of the anode was very small. On the other hand, coarsening of TZ8Y and Ni/TZ8Y cermet powders had a profound effect on the performance of Ni/TZ8Y cermet anodes. The best performance was found to be the Ni/TZ8Y cermet anodes prepared from Ni/TZ8Y cermet powder previously coarsened at 1300°C. Sintering Ni/zirconia cermet anodes at high temperatures (*e.g.*, 1400°C) was essential to reduce both the electrode ohmic resistance and electrode polarization resistance. The results demonstrated that the sintering behavior of the zirconia phase in the cermets affect not only the formation of zirconia-to-zirconia ionic network but also the formation of the Ni-to-Ni electrical network of the Ni/zirconia cermet anodes and thus the electrical contact between the Ni phase in the cermet and YSZ electrolyte.
 [DOI: 10.1149/1.1612505]

Manuscript submitted October 9, 2002; revised manuscript received May 12, 2003. Available electronically September 19, 2003.

In solid oxide fuel cells (SOFCs), the principal anode materials are Ni/Y_2O_3-ZrO_2 (Ni/YSZ) cermets due to their high electrochemical performance and high stability at SOFC operation conditions.[1-12] Nickel is know to have high electrocatalytic activity for the H_2 oxidation reaction[13,14] and is also available in abundance. The addition of Y_2O_3-ZrO_2 (YSZ) in the Ni cermet electrodes significantly improves the thermal compatibility of the cermet electrodes with the YSZ electrolyte, reduces the sintering and agglomeration of Ni and increases the electrochemical activity of the cermet electrodes.[4-6] The electrochemical performance of Ni/YSZ cermet anodes is strongly affected by the microstructure and the distribution of Ni and YSZ phases of the electrodes. This in turn is dependent on the powder synthesis and electrode fabrication processes, such as the particle-size distribution of NiO and YSZ powders and heat-treatment of NiO, YSZ, and Ni/YSZ cermet powders.[7-12,15] The presence of the YSZ phase in the cermets not only inhibits the sintering and growth of the Ni phase but also actively promotes the electrochemical and catalytic activity of the anodes by extending the reaction zones or the three-phase boundary (where electrode, electrolyte, and fuel gas reactant meet). De Boer *et al.* studied the electrochemical performance of porous Ni electrodes modified by deposition with fine YSZ powder and showed that the presence of fine YSZ particles on the Ni electrode surface creates additional active sites for the H_2 oxidation reaction.[8] Our recent study shows that addition of nanosized YSZ and Sm-doped CeO_2 particles into Ni/YSZ cermet anode structure by the ion impregnation method substantially increases the electrochemical activity of the Ni/YSZ cermet anodes for the H_2 oxidation reaction.[16] On the other hand, there is evidence that the optimization of the fabrication process parameters may depend strongly on the nature of the Y_2O_3-ZrO_2 phase in the cermet. Kawada *et al.* investigated the performance of Ni/8 mol % Y_2O_3-ZrO_2 (Ni/TZ8Y) fabricated by slurry painting and found that coarsening Ni/TZ8Y cermet powder at temperatures as high as 1400°C was essential for reducing the electrode resistance and for achieving high electrode performance.[7] Van Berkel *et al.* reported the best electrode performance of Ni/TZ8Y cermet anodes prepared from TZ8Y powder coarsened at 1500°C.[17] Coarsening was also reported to be effective for creating a stable and active Ni/TZ8Y cermet microstructure combining coarse (27 μm) and fine (0.6 μm) TZ8Y grains for the H_2 oxidation reaction.[18] Very different from the Ni/TZ8Y cermet anodes, a recent study on the fabrication process of Ni/3 mol % Y_2O_3-ZrO_2 (Ni/TZ3Y) cermet anodes showed that the coarsening treatment of TZ3Y or Ni/TZ3Y cermet powders has little effect on the electrode performance and large TZ3Y particles are actually detrimental to the electrocatalytic activity of the Ni/TZ3Y cermet anodes.[19] The different responses of Ni/TZ8Y and Ni/TZ3Y cermet anodes in relation to the coarsening treatment of zirconia and Ni/zirconia cermet powder may be related to the very different sintering behavior of tetragonal (*e.g.*, TZ3Y) and cubic (*e.g.*, TZ8Y) zirconia materials, as shown by Cutler *et al.*[20]

To clarify the role of the sintering behavior of zirconia in the fabrication processes and performance of Ni/zirconia cermet electrodes, the fabrication process and electrode performance of Ni/TZ3Y and Ni/TZ8Y cermet systems were investigated under identical experimental conditions. The results indicate that the fabrication process of Ni/zirconia cermet electrodes depends critically on the sintering properties of zirconia powders in the cermets.

Experimental

Electrolyte substrates were prepared from 3 mol % Y_2O_3-ZrO_2 (TZ3Y, Tosoh, Japan) and 8 mol % Y_2O_3-ZrO_2 (TZ8Y, Tosoh, Japan) by isopress, followed by sintering at 1500°C for 4 h in air. The electrolyte thickness was controlled at 0.90 ± 0.03 mm and the diameter was ~19 mm. Based on the electrolyte thickness and reported conductivity value, the ohmic resistance for TZ3Y and TZ8Y electrolyte substrates was calculated to be ~1.5 and ~0.5 Ω cm^2 at 1000°C, respectively.[21] TZ3Y and TZ8Y powders were used to prepare Ni/TZ3Y and Ni/TZ8Y cermets. Coarsening of TZ3Y and TZ8Y powders was carried out at temperatures ranging from 1000 to 1400°C for 5 h in air. Ni/TZ3Y cermet powders with composition of Ni (70 vol %)/TZ3Y (30 vol %) were prepared by mixing TZ3Y and NiO (Ajax, Australia) powders by a ballmill in propanol using TZ3Y grinding medium for 3 h, followed by drying and sieving. The color of NiO powder was dark gray to black. In the case of coarsening treatment of cermet powders, the cermet powders after the ballmilling process were coarsened at selected temperatures (1200 to 1400°C) for 5 h in air and the powder was then ballmilled again for 3 h. Slurry of cermet powders was prepared by extensive grinding of the powder with the addition of triethyleneglycol. Ni/TZ8Y slurry with composition of Ni (50 vol %)/TZ8Y (50 vol %) was prepared in the same way. The coarsening treatment of Ni/TZ8Y cermet powders was similar to that for the Ni/TZ3Y cermet powders. Electrodes were applied onto zirconia substrates by slurry painting, followed by sintering at 1400°C for 2 h in air. The sintering temperature of

[z] E-mail: mspjiang@ntu.edu.sg

Ni/zirconia cermet anodes was also studied at temperatures ranging from 1100 to 1500°C for 2 h in air. TZ3Y electrolyte substrates were used for Ni/TZ3Y cermet electrodes and TZ8Y electrolyte substrates were used for Ni/TZ8Y cermet electrodes. The electrode coating thickness was in the range of 20 to 40 μm, and the electrode area was in the range of 0.35 to 0.4 cm^2.

Pt paste (Engelhard 6082) was applied to the opposite side of the electrode to make counter and reference electrodes. The counter electrode was in the center of the electrolyte substrate opposite the cermet electrode, and the reference electrode was a ring around the counter electrode. The counter and working electrodes were geometrically symmetrical. Fine Pt mesh was used as the current collector for both the cermet electrode and counter electrode. The anode side of the cell was sealed with a Pyrex glass ring. Hydrogen gas (99.98%, BOC) was used as fuel and air as the oxidant. Water vapor (~3%) was introduced into hydrogen fuel through a gas bubbler in a temperature-controlled water bath. The flow rate of humidified hydrogen gas was 100 mL min^{-1}. The cathode side of the cell was exposed to air. The test cell configuration has been given elsewhere.[14] Under test conditions of 1000°C and 97% H_2/3% H_2O, the open-circuit potential of the cell generally varied between 1.070 to 1.080 V against the Pt air reference electrode. The hydrothermal degradation of tetragonal ZrO_2 to monoclinic ZrO_2 usually occurs when annealed at relatively low temperatures (65-400°C) in the presence of water vapor.[22,23] However, at fuel cell test conditions of 1000°C and 97% H_2/3% H_2O, tetragonal ZrO_2 phase is quite stable as demonstrated by the long-term stability of TZ3Y cells.[19] The electrochemical performance of the cermet anodes was measured by galvanostatic current interruption (GCI) and electrochemical impedance spectroscopy (EIS). GCI was carried out in a fuel cell operation mode (*i.e.*, the cell generates current to the external circuit). EIS was measured under open circuit in a frequency range of 1 to 100 kHz under an amplitude of 5 mV using a Voltech frequency responses analyzer (FRA, TF2000) in conjunction with a potentiostat. Overpotential (η) and IR losses were directly measured from GCI curves. Electrode ohmic resistance (R_Ω) was obtained from the slopes of plots of IR losses *vs.* current densities.[19] From EIS spectra, the difference in the high and low frequency intercepts gives the electrode polarization (interface) resistance (R_E) which is generally associated with the electrochemical activity of the electrode. Without specification, the polarization curves (*i.e.*, *V-j* curves) were the overall polarization performance of the anodes for the H_2 oxidation reaction, which included both the η components and IR losses. As electrode ohmic resistance (R_Ω) was measured between the anode and the Pt air reference electrode, R_Ω includes resistive contributions of electrode and electrolyte. As the thickness of the electrolyte substrates was kept relatively constant (0.90 ± 0.03 mm), any significant variation of R_Ω as compared to the calculated value of the electrolyte substrate would be an indication of the electrical contact between the electrode and electrolyte and the conductivity of the porous cermet electrode coatings. The microstructure and morphology of the anodes were examined by scanning electron microscopy (SEM). All Ni/zirconia cermet electrodes were reduced *in situ* in the fuel cell test station before the EIS and GCI measurements.

The particle size and particle size distribution of NiO, TZ3Y, and TZ8Y powders were measured by a sedimentation method using a SediGraph 5000ET particle size analyzer (Micromeritics, USA). Powders were first dispersed by ballmilling for 3 h which was followed by an ultrasonic bath treatment for ~1 h before the measurement. The particle-size measurement was repeated until reproducible distribution curves were obtained. Average particle size of the powders was measured by the d_{50} value from the particle-size distribution curves. The particle size was also estimated from transmission electron microscopy (TEM) and SEM in some cases.

Results

Average particle size and particle size distribution of the powders.—Figure 1 shows particle-size distribution curves of as-received TZ3Y, TZ8Y, and NiO powders. From the distribution curves, the average particle size of TZ3Y, TZ8Y, and NiO powders was estimated to be ~0.30, ~0.36, and ~1.0 μm, respectively. From TEM, the average particle size estimated was ~0.03 μm for NiO and ~0.06 μm for TZ3Y and TZ8Y. The average particle size determined by TEM is smaller than that estimated from SediGraph measurement. The reason could be due to the fact that the sedimentation method probably measures the particle-size distribution of agglomerates of zirconia powders rather than the individual particles. The characteristics of the particle-size distribution and average particle size of starting TZ3Y and TZ8Y powders were very similar, showing very fine particles and a more symmetrical distribution as compared to NiO. In fact, the specific surface area of these two commercial powders was very close (~15.8 to 15.9 m^2 g^{-1}).[21] However, the effects of the coarsening temperature on the particle size and particle-size distribution are somewhat different on NiO, TZ3Y, and TZ8Y powders. The as-received NiO powder had very

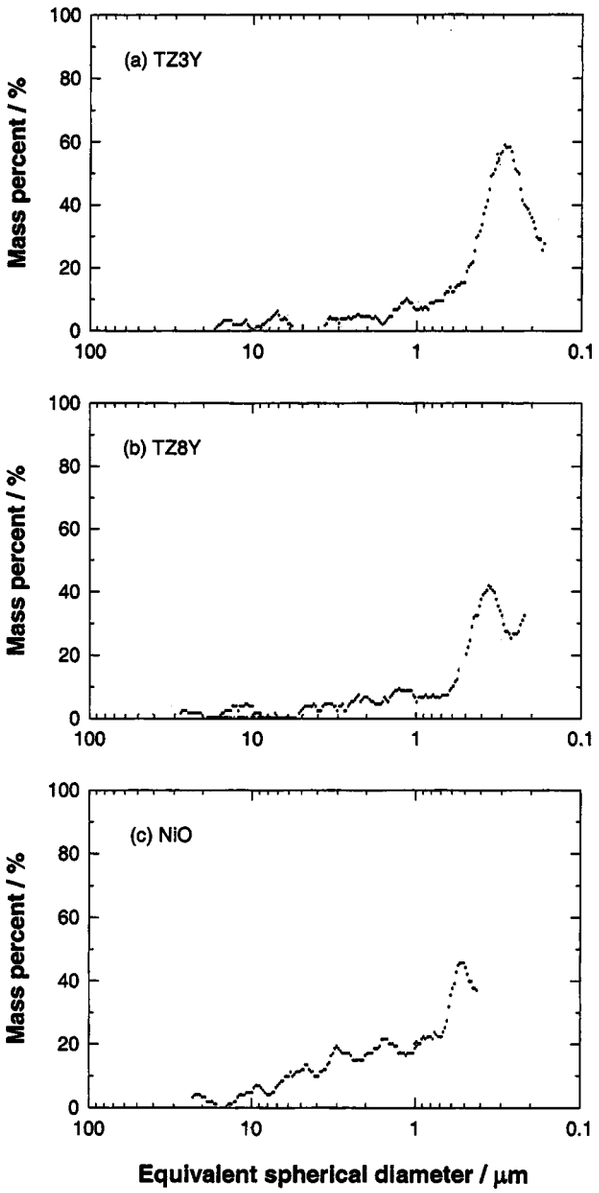

Figure 1. Particle size distribution curves of as-received TZ3Y, TZ8Y, and NiO powders.

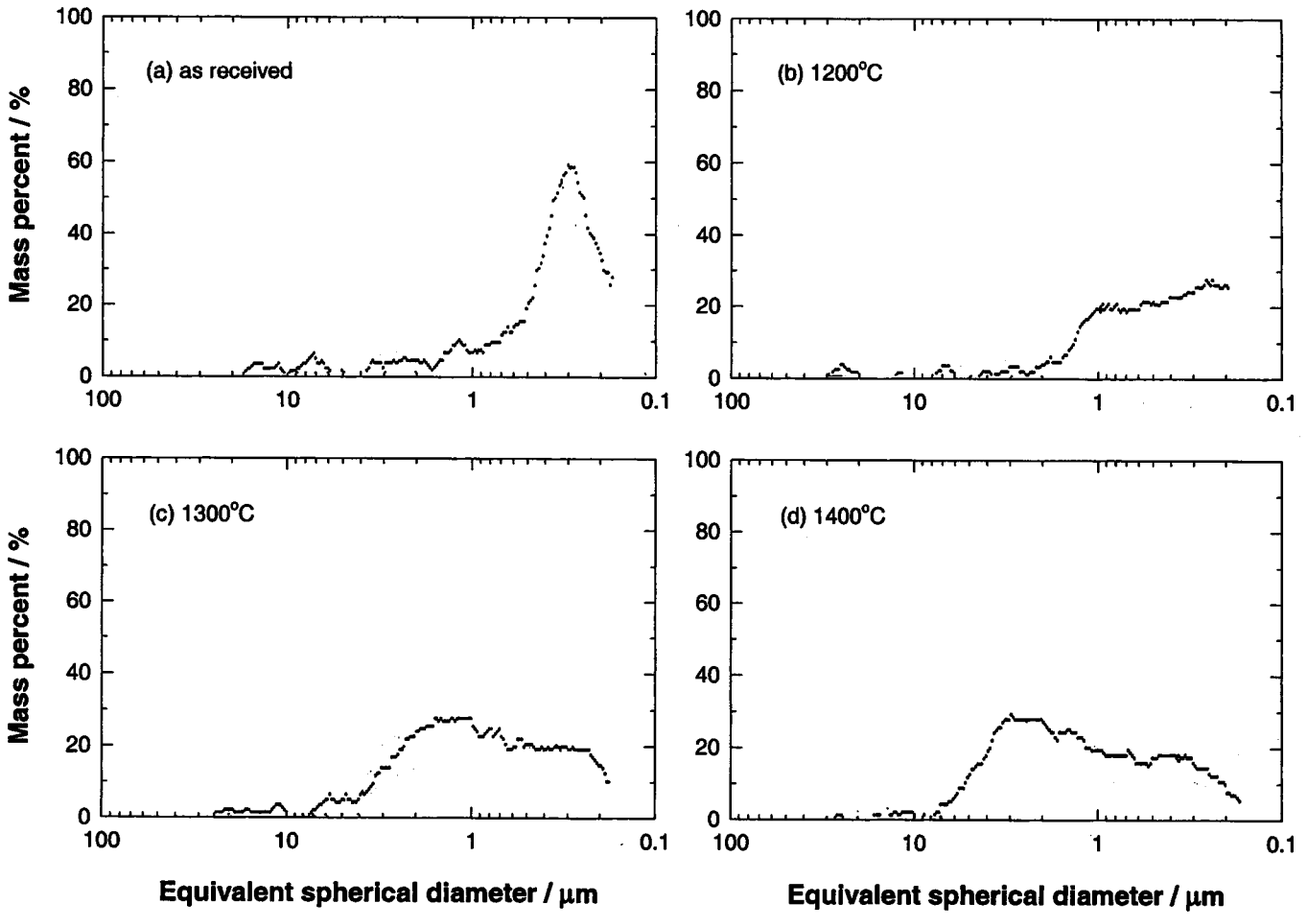

Figure 2. Particle size distribution curves of TZ3Y powder coarsened at different temperatures for 5 h.

fine particles with a broad particle-size distribution. As shown earlier,[19] coarsening NiO increased the particle size and the particle-size distribution became more symmetrical. For example, the average particle size of NiO increased to 4.8 μm after the heat-treatment at 1100°C. Similar to that observed for the NiO, there were also changes in both the particle-size distribution and the particle size for TZ3Y powder. Figure 2 shows the particle-size distribution of TZ3Y powder coarsened at different temperatures. The average particle size was 1.42 μm for TZ3Y powder coarsened at 1400°C as compared to 0.30 μm of as-received TZ3Y powder. From TEM micrographs, the average particle size of TZ3Y powders coarsened at 1400°C was estimated to be 0.39 μm. The distribution of TZ3Y powders also became broader after the coarsening treatment. For TZ8Y powders, the measurement of the particle size distribution by the sedimentation method was found to be difficult after the coarsening treatment of the TZ8Y powder. Figure 3 shows the particle-size distribution curves of as-received TZ8Y powder and TZ8Y powder coarsened at 1200°C. There was a marked change in the particle-size distribution of TZ8Y powder after coarsening treatment. It was no longer feasible to measure accurately the average particle size of the TZ8Y powder from the distribution curves after coarsening treatment at 1200°C due to the significant precipitation taking place during the measurement. The significant grain growth and agglomeration of TZ8Y particles can also be seen from the SEM examination. Figure 4 shows the SEM pictures of the TZ8Y powder coarsened at different temperatures. For comparison, TZ8Y powder before the coarsening treatment is also shown in the figure. The primary particle size of as-received TZ8Y powders was 0.06 μm and after coarsening at 1200°C, the particles grew to 20 to 30 μm in size and the formation of agglomerates was evident. Some of the agglomerates could be broken with the ballmilling method used in the present study. At a coarsening temperature of 1400°C, hard agglomerates of ~30 μm were formed and were difficult to break by the ballmilling method used. Figure 5 compares the average particle size of NiO, TZ3Y, and TZ8Y powders coarsened at different temperatures, as measured by the SediGraph method. The grain growth of TZ8Y powder is much faster and more pronounced as compared to that of TZ3Y and NiO powders. The results also showed that the

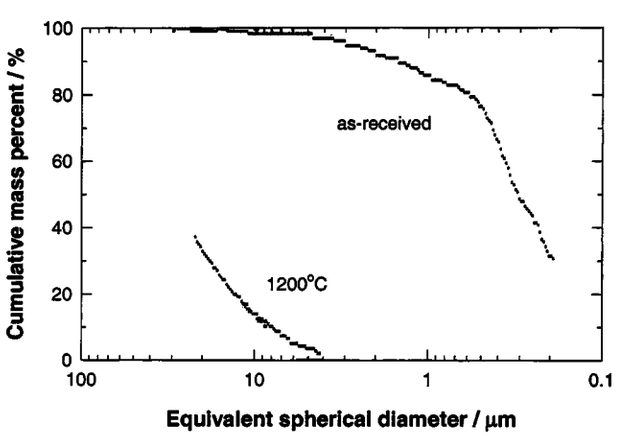

Figure 3. Particle size distribution curves of as-received TZ8Y powder and TZ8Y powder coarsened at 1200°C for 5 h in air.

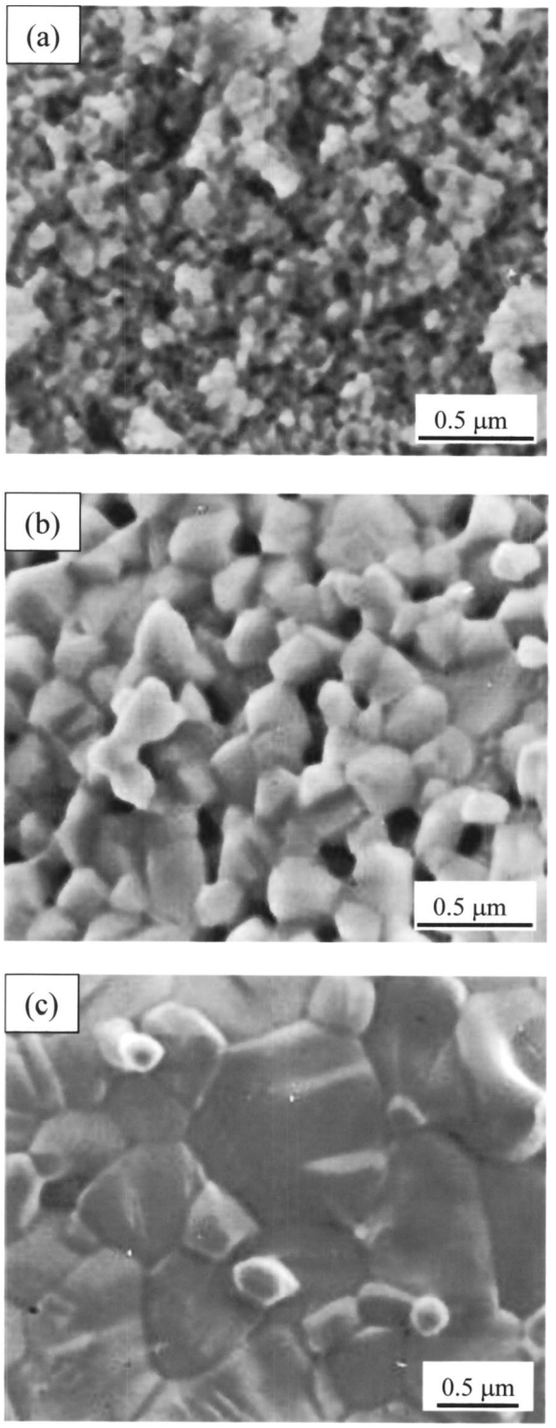

Figure 4. SEM pictures of the TZ8Y powder coarsened at different temperatures for 5 h in air: (a) as-received, no coarsening, (b) 1100°C, and (c) 1300°C.

ballmilling method used in the present study was not effective enough to break the hard agglomerates which formed.

Effect of coarsening treatment of zirconia powders.—Figure 6 shows the polarization and impedance performance of Ni (70 vol %)/TZ3Y (30 vol %) anodes. The anodes were prepared from as-received TZ3Y powders and TZ3Y powders coarsened at 1400°C for 5 h in air. The sintering temperature of the anodes was 1400°C

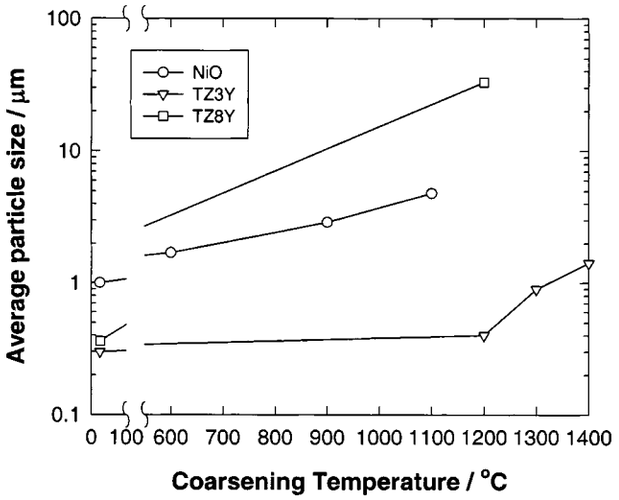

Figure 5. Average particle size of NiO, TZ3Y, and TZ8Y powders coarsened at different temperatures. The particle size distribution was determined by the SediGraph method. The lines are to guide the eyes only.

for 2 h. There was a reduction in the overall polarization performance of Ni/TZ3Y cermet anodes prepared from TZ3Y powder coarsened at 1400°C as compared with that prepared from as-received TZ3Y powders. As shown by the impedance curves (Fig. 6b), coarsening TZ3Y at 1400°C increased electrode polarization resistance (R_E) to 2.83 Ω cm^2 as compared to 0.59 Ω cm^2 for the anode prepared from as-received TZ3Y powders while there was no

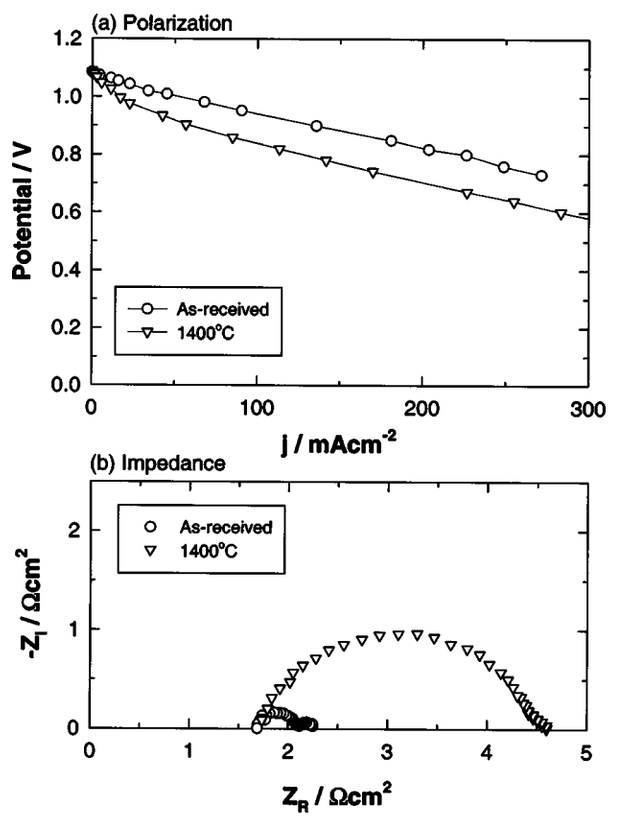

Figure 6. Polarization and impedance performance of Ni (70 vol %)/TZ3Y (30 vol %) anodes prepared from as-received TZ3Y powder and TZ3Y powder coarsened at 1400°C, measured at 1000°C.

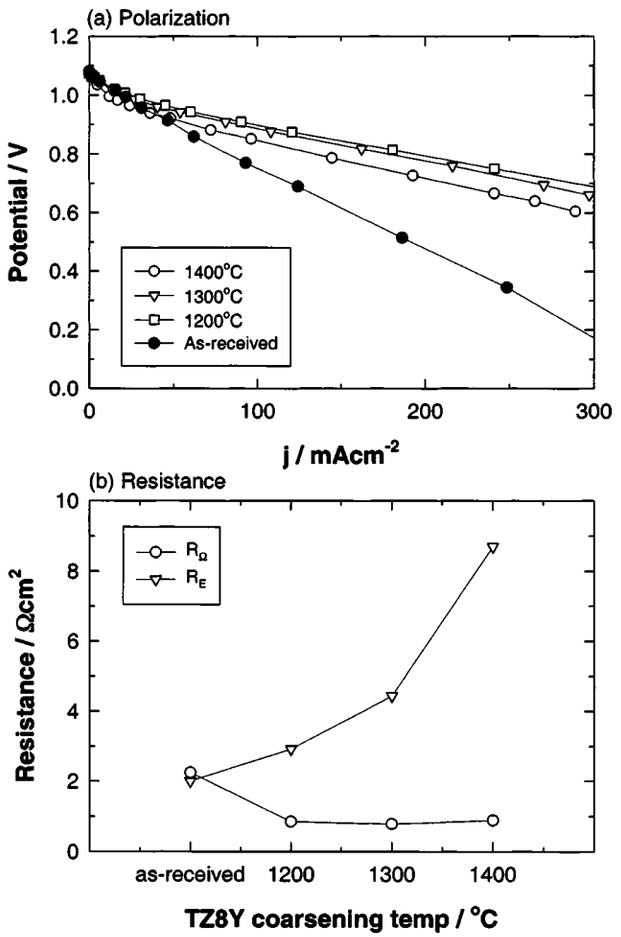

Figure 7. Polarization performance and electrode ohmic and polarization resistances of Ni (50 vol %)/TZ8Y (50 vol %) cermet anodes as a function of coarsening temperatures of TZ8Y powders, measured at 1000°C.

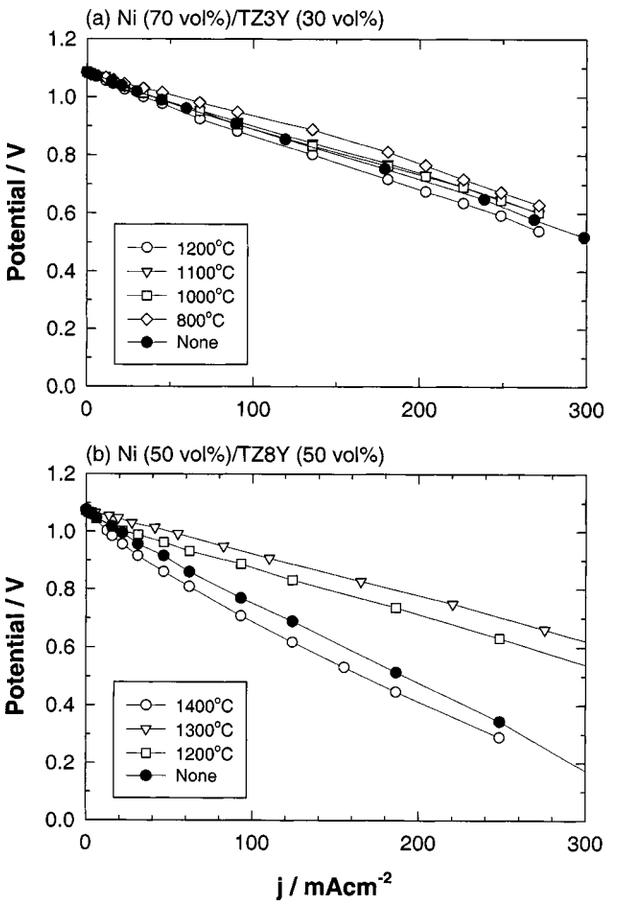

Figure 8. Effect of coarsening temperatures of Ni/zirconia cermet powders on the polarization performance of (a) Ni (70 vol %)/TZ3Y (30 vol %) and (b) Ni (50 vol %)/TZ8Y (50 vol %) cermet anodes, measured at 1000°C.

change in the ohmic resistance (R_Ω) of the anode. The increase in the R_E is most likely related to the increase in the particle size of TZ3Y powders (Fig. 2), leading to the overall reduction of the three-phase boundary areas of the Ni/TZ3Y cermet anodes.

In contrast to the coarsening treatment of TZ3Y powder, the effect of coarsening TZ8Y powders on the electrochemical performance of Ni/TZ8Y anodes appears more complicated. Figure 7 shows polarization performance and electrode ohmic and polarization resistances of Ni (50 vol %)/TZ8Y (50 vol %) cermet anodes as a function of coarsening temperatures of TZ8Y powders. The anodes were finally sintered at 1400°C. The overall polarization performance was improved for the anodes prepared from TZ8Y powder after the coarsening treatment (*e.g.*, at 1200°C) as compared to that prepared from as-received TZ8Y powder. Coarsening treatment of TZ8Y powders not only affects the electrode polarization resistance but also the electrode ohmic resistance. However, the improvement of the anode performance was primarily due to the significant effect of the coarsening treatment of TZ8Y powders on the electrode ohmic resistance. R_Ω decreased from 2.24 Ω cm^2 for the anode prepared from as-received TZ8Y powder to 0.8 to 0.9 Ω cm^2 for the Ni/TZ8Y anodes after the coarsening treatment of TZ8Y powder at 1200 to 1400°C. In contrast to R_Ω, electrode polarization resistance for the H_2 oxidation reaction increases with an increase in the coarsening temperature of TZ8Y powder. R_E increased from 2.0 Ω cm^2 for the anode prepared from as-received TZ8Y powder to 4.48 and 8.7 Ω cm^2 for the anode prepared from TZ8Y powders coarsened at 1300 and 1400°C, respectively. As shown above, for TZ8Y powders coarsened at temperatures higher than 1200°C, hard and large agglomerates were formed, and some of them were still intact after milling. Thus, the significant grain growth and the existence of large agglomerates would reduce the three-phase boundaries of the anode and thus increase electrode polarization resistance (R_E) for the reaction. This is similar to the effect of particle size of TZ3Y on the performance of the Ni/TZ3Y cermet anode.[19] Nevertheless, the results indicate that unlike the Ni/TZ3Y cermet anodes, reducing the sintering process of the TZ8Y phase in the Ni/TZ8Y cermets through the coarsening treatment of TZ8Y powder would be effective for improving the electrode conductivity of the Ni/TZ8Y cermet anodes. Coarsening TZ8Y powder was also used by van Herle *et al.* to control the particle-size distribution of the zirconia powder in the cermet.[24]

Effect of coarsening treatment of Ni/zirconia cermet powders.—Figure 8 shows the effect of coarsening treatment of Ni/zirconia cermet powders on the polarization performance of Ni (70 vol %)/TZ3Y (30 vol %) and Ni (50 vol %)/TZ8Y (50 vol %) cermet anodes. The sintering temperature of the anode was 1400°C. For Ni/TZ3Y cermet anodes, the effect of coarsening treatment of the cermet powder on the overall electrode performance is relatively small. However, it was found that coarsening Ni/TZ3Y cermet powder can reduce the formation of surface cracks of the electrode coating and improve the coating quality, as shown in Fig. 9. Coarsening the Ni/TZ3Y cermet powder at 1200°C significantly reduced the formation of surface cracks of the cermet coating, and this is most likely due to the reduced shrinkage of the cermet powder. The improvement of the surface quality of Ni/TZ3Y cermet anodes can also

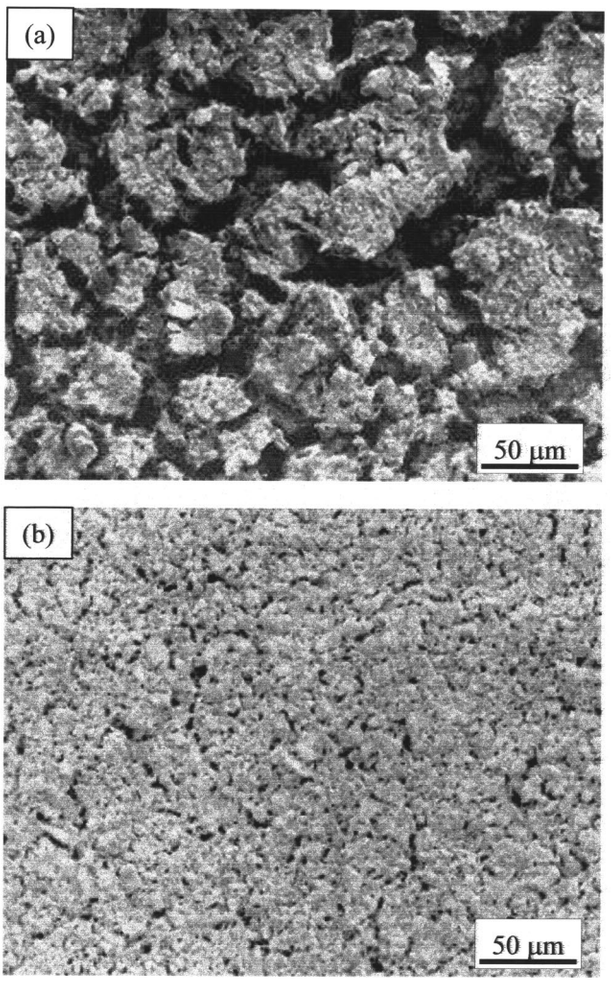

Figure 9. SEM picture of the Ni (70 vol %)/TZ3Y (30 vol %) cermet coating of the anode prepared from cermet powder (a) without coarsening and (b) after coarsening at 1200°C.

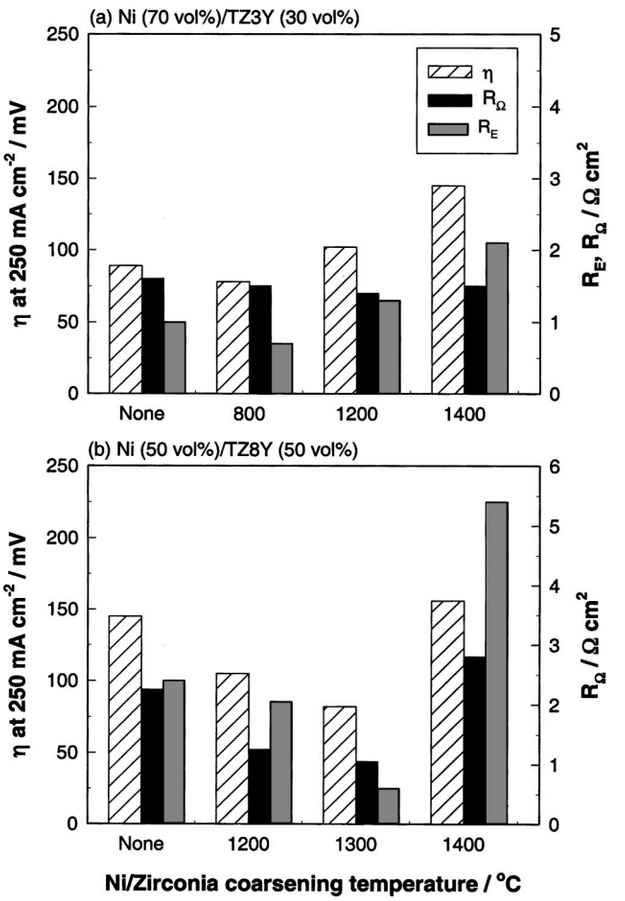

Figure 10. Effect of coarsening temperature of the Ni/zirconia cermet powder on the electrode performance of (a) Ni (70 vol %)/TZ3Y (30 vol %) and (b) Ni (50 vol %)/TZ8Y (50 vol %) cermet anodes, measured at 1000°C.

be achieved by a coarsening treatment of the NiO powders alone.[19] In contrast, the effect of coarsening of the cermet powder on the electrode performance of Ni/TZ8Y cermet anodes is significant. The best performance of Ni/TZ8Y cermet anodes was obtained on the anode prepared from cermet powder coarsened at 1300°C (Fig. 8b). The dependence of the electrode performance of Ni/TZ3Y and Ni/TZ8Y cermet anodes on the coarsening temperature of the cermet powder can be seen more clearly from the change of the electrode performance as a function of the coarsening temperatures, as shown in Fig. 10. Coarsening Ni/TZ3Y cermet powder essentially had no effect on the electrode's ohmic resistance. However, a high coarsening temperature of Ni/TZ3Y cermet powder would be detrimental to the electrode performance as indicated by the small increase of R_E. On the other hand, coarsening Ni/TZ8Y cermet powder reduced both R_E and R_Ω of the anode. For the Ni/TZ8Y cermet anode prepared from the cermet powder coarsened at 1300°C, R_Ω and R_E were 1.07 and 0.6 Ω cm^2, respectively, much lower than 2.24 and 2.4 Ω cm^2 of the anode prepared from cermet powder without coarsening treatment. Increasing the coarsening temperature to 1400°C (the same temperature as the sintering temperature of anodes), R_Ω increased to 2.77 Ω cm^2 again. The same trend was also found for the electrode polarization resistance. R_Ω and R_E were the lowest for the anodes prepared from the Ni/TZ8Y cermet powder coarsened at 1300°C. This indicates that for the Ni/TZ8Y cermet anodes sintered at 1400°C, the optimum coarsening temperature for the cermet powders would be ~1300°C for the electrode to have minimum electrode ohmic resistance and electrode polarization resistance. In the case of Ni (40 vol %)/TZ8Y (60 vol %) cermet anodes, Kawada *et al.*[7] observed the best performance of R_Ω = 0.56 Ω cm^2 and R_E = 0.29 Ω cm^2 as measured at 1000°C in wet hydrogen for the Ni/TZ8Y cermet anodes prepared with a cermet powder coarsening temperature of 1400°C and an anode sintering temperature of 1500°C. However, when the anode sintering temperature decreased to 1400°C (the same temperature as the cermet coarsening temperature), both R_Ω and R_E increased significantly to 2.27 and 2.55 Ω cm^2, respectively. The effect of coarsening treatment of Ni/TZ8Y cermet powders on the performance of the Ni (50 vol %)/TZ8Y (50 vol %) anode in the present study agrees very well with that reported by Kawada *et al.*[7]

Effect of anode sintering temperature.—Figure 11 shows polarization and impedance curves of Ni (70 vol %)/TZ3Y (30 vol %) cermet anodes sintered at different temperatures, measured at 1000°C. The anodes were prepared from TZ3Y powders without coarsening treatment. The effect of the anode sintering temperature on electrode performance of Ni/TZ3Y cermet anodes is remarkable. The polarization performance of the cermet anodes increased significantly with the sintering temperature of anodes as shown in Fig. 11a. For the Ni/TZ3Y anodes sintered at 1100 and 1400°C, two impedance arcs were observed at low and high frequencies. The impedance arcs at both high and low frequencies of the anode sintered at 1400°C were much smaller than that sintered at 1100°C. R_E for the H_2 oxidation was 36.5 Ω cm^2 for the anode sintered at

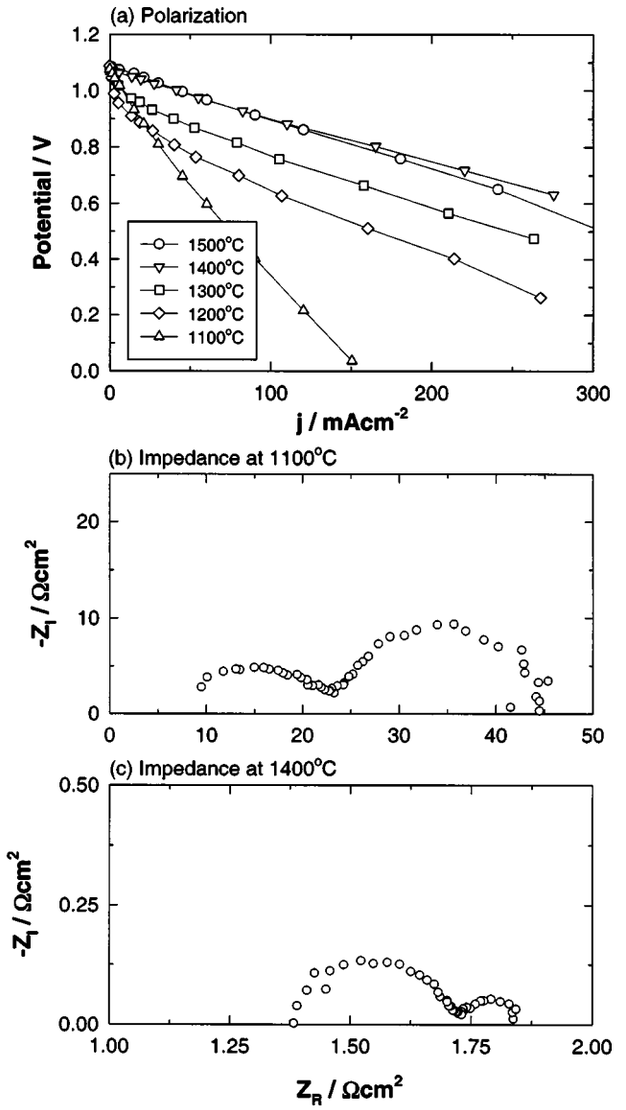

Figure 11. (a) Polarization curves of Ni (70 vol %)/TZ3Y (30 vol %) cermet anodes sintered at different temperatures and impedance curves of the anode sintered at (b) 1100°C and (c) 1400°C. Polarization and impedance curves were measured at 1000°C.

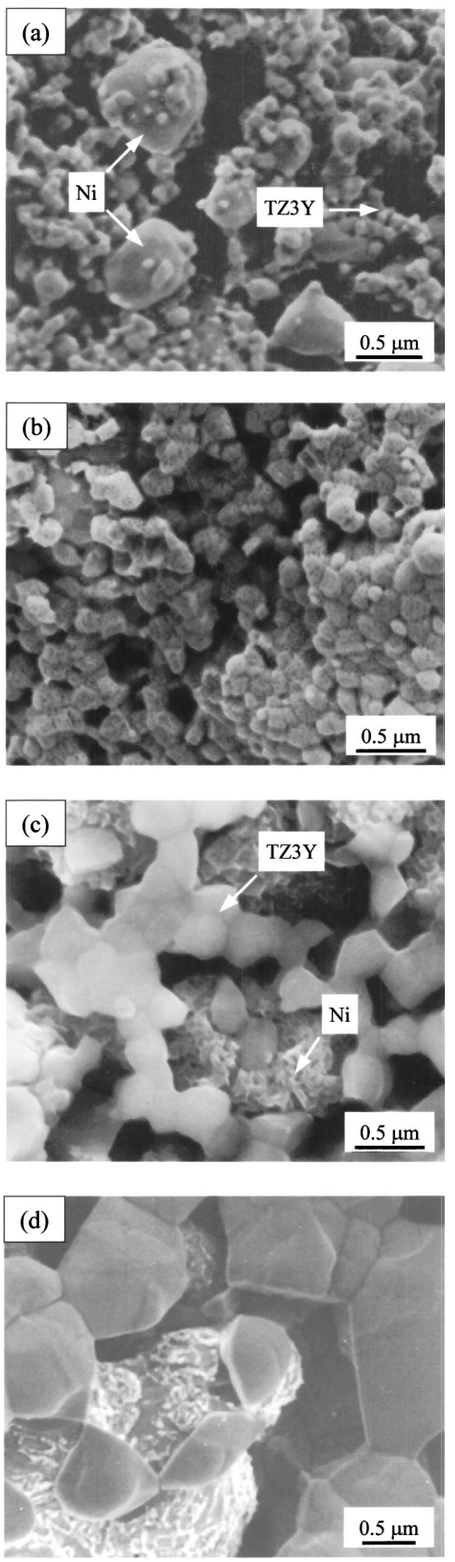

Figure 12. SEM pictures of the Ni (70 vol %)/TZ3Y (30 vol %) cermet anodes sintered at (a) 1100, (b) 1300, (c) 1400, and (d) 1500°C after fuel cell testing.

1100°C and decreased significantly to 0.45 Ω cm^2 when the sintering temperature of the anode increased to 1400°C. Most important, the increase of the anode sintering temperature from 1100°C to 1400°C also significantly decreased the electrode ohmic resistance. R_Ω was reduced from 8.5 Ω cm^2 for the anode sintered at 1100°C to 1.37 Ω cm^2 for that sintered at 1400°C. The dramatic reduction in R_E and R_Ω with the increase in the anode sintering temperature was also observed for the Ni/TZ3Y cermet anodes with Ni content of 50 vol %.[19] This indicates that the establishment of an effective Ni-to-Ni electronic and zirconia-to-zirconia ionic networks in the cermet depends strongly on the sintering temperature of the anodes. The appearance of two separable impedance arcs indicates that there are at least two limiting electrode processes for the H_2 oxidation reaction on Ni/zirconia cermet anodes.[6]

Figure 12 shows the SEM picture of the Ni (70 vol %)/TZ3Y (30 vol %) cermet anodes sintered at different temperatures. The microstructure of the anodes was generally characterized by large Ni particles surrounded by much smaller TZ3Y particles. Ni particles grow significantly as the anode sintering temperature increases. On the other hand, there is a clear development of a TZ3Y phase from loosely contacted particles to an intimately bonded and continuous network of TZ3Y particles as the anode sintering temperature in-

creases. For Ni/TZ3Y cermet anodes sintered at 1100°C, there was very little sintering taking place for TZ3Y powders and TZ3Y particles were very small (Fig. 12a). For the anodes sintered at 1300°C, the TZ3Y phase still does not appear fully sintered and in loose contact, indicated by the fine pores on the surface of TZ3Y grains (Fig. 12b). As shown in Fig. 12c, sintering of the TZ3Y phase occurred at the temperature of 1400°C. This is indicated by the significant grain growth and the development of the strong and intimate bonding between the TZ3Y grains. Such strong bonding would also be expected to occur between the TZ3Y phase in the cermet and TZ3Y electrolyte at the electrode and electrolyte interface.[25] Therefore, sintering of the zirconia phase at temperatures of around 1400°C is essential to form a TZ3Y-to-TZ3Y ionic network, which in turn would lead to the formation of a Ni-to-Ni electronic network. This is supported by the simultaneous reduction in the electrode ohmic resistance and electrode polarization resistance of Ni/TZ3Y cermet anodes with the increase of the sintering temperatures (Fig. 11). Sintering at a higher temperature (*e.g.*, 1500°C, Fig. 12d) resulted in the substantial increase in both Ni and TZ3Y particles and had a detrimental effect on the electrode performance. It was also found that the adherence of the coatings sintered at temperatures higher than 1200°C was much stronger than those sintered at lower temperatures.

Similar to the Ni/TZ3Y cermet anodes, the polarization performance of Ni/TZ8Y cermet anodes strongly depends on the sintering temperature of the anode. Moreover, the effect of the anode sintering temperature on the polarization performance of Ni/TZ8Y cermet anodes appears to be related to the coarsening temperature of the cermet powder. Figure 13 shows the polarization performance and the corresponding electrode ohmic resistance and polarization resistance of the Ni (50 vol %)/TZ8Y (50 vol %) cermet anodes sintered at different temperatures. The anodes were prepared from Ni/TZ8Y cermet powder coarsened at 1300°C. For the anodes sintered at temperatures close to the coarsening temperatures of the cermet powder (in this case, it is ~1300°C), the electrochemical performance of the anode was very poor (see Fig. 13a). Increasing the sintering temperature to 1400°C improves the electrode performance substantially. This can also be seen for the change of the electrode ohmic and polarization resistances with the sintering temperature. R_Ω and R_E were 8.6 and 17.5 Ω cm^2, respectively, for the anode sintered at 1300°C, the same temperature as the Ni/TZ8Y cermet coarsening temperature. After sintering at 1400°C, R_Ω and R_E values were reduced to 1.03 and 0.75 Ω cm^2, respectively, significantly lower than that for the anode sintered at 1300°C. This indicates that a high sintering temperature as compared to the coarsening temperature of the cermet powder would be needed to achieve low electrode ohmic resistance and low polarization resistance and thus high electrode performance of Ni/TZ8Y cermet anodes. However, further increasing the anode sintering temperature to 1500°C had little positive effect on the electrode performance, similar to that observed for Ni/TZ3Y cermet anodes. Figure 14 shows the SEM pictures of the Ni/TZ8Y cermet anodes sintered at different temperatures. Similar to those observed on the Ni/TZ3Y cermet anodes, for the anodes sintered at temperatures lower than 1400°C, the TZ8Y grains appear to be loosely contacted (Fig. 14a and b). This would result in the poor Ni-to-Ni and TZ8Y-to-TZ8Y networking, indicated by the high R_Ω and R_E values. For the Ni/TZ8Y anodes sintered at 1400°C, TZ8Y grains grew to 0.5 to 2 μm, and an intimate and continuous network between TZ8Y particles was developed. From the microstructural point of view, the effect of the sintering temperature on the development of Ni-to-Ni and TZ8Y-to-TZ8Y networks for Ni/TZ8Y cermet anodes is very similar to that observed on the Ni/TZ3Y cermet anodes despite the significant difference in the Ni content in the Ni/TZ8Y and Ni/TZ3Y cermets studied.

To further clarify the effect of the sintering temperature on electrode performance and in particular on the electrode ohmic resistance of the Ni/zirconia cermet anode, pure Ni anodes prepared from NiO powders were studied. Figure 15 is the polarization and impedance curves of Ni anodes sintered at different temperatures, measured at 1000°C. The electrode performance of Ni anodes also increases with the increase in anode sintering temperature. However, the effect of the anode sintering temperature on the polarization performance of Ni anodes is much smaller as compared to that on the Ni/TZ3Y and Ni/TZ8Y cermet anodes (see Fig. 11 and 13). Most interesting, the R_Ω of Ni anodes sintered at 1100 to 1500°C was in the range of 1.63 to 1.43 Ω cm^2 (Fig. 15c). Some variation in R_Ω is most likely due to the variation in YSZ electrolyte thickness. This indicates that the electrode ohmic resistance of pure Ni anodes is essentially independent of the anode sintering temperature, in contrast to those of Ni/TZ3Y and Ni/TZ8Y cermet anodes. This result clearly demonstrated that the dependence of the electrode ohmic resistance of the Ni/zirconia cermet anodes on the anode sintering temperature is related to the sintering effect of the zirconia phase in the cermet on the formation of a Ni-to-Ni electrical network. The improvement in the electrode performance of the Ni anode with increasing sintering temperature is solely due to the reduction in the electrode polarization resistance, as shown in Fig. 15b. The higher anode sintering temperature led to the lower R_E (Fig. 15c). It is not clear at this stage why R_E was reduced at high sintering temperatures as there was an increase in the Ni grains with the increase in the anode sintering temperature. One of the reasons could be related to the complexity in the microstructure and impurity distribution at the metallic Ni and YSZ electrolyte interfaces.[26,27] The high sintering temperature may be beneficial for reducing the impurities at the

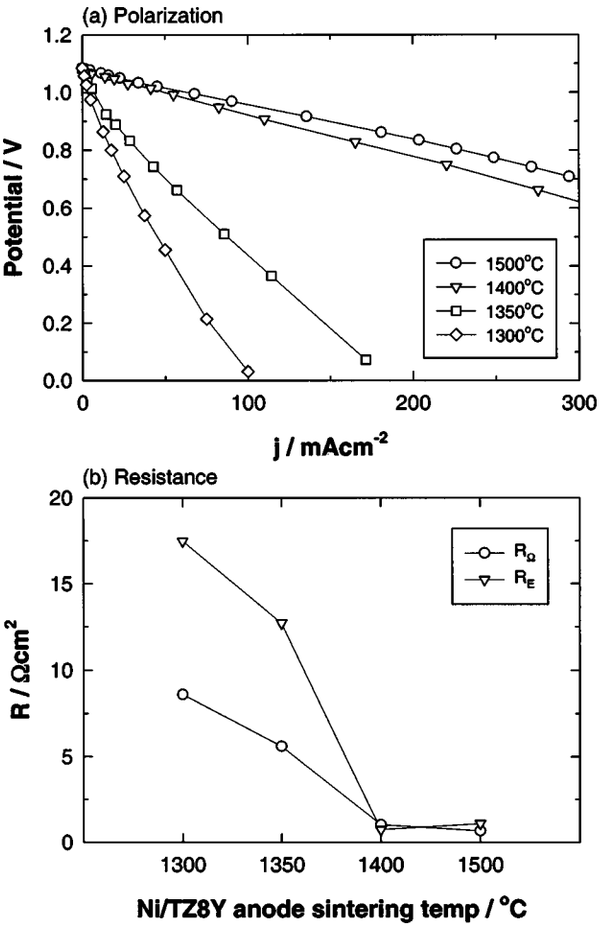

Figure 13. (a) Polarization and (b) resistance curves of Ni (50 vol %)/TZ8Y (50 vol %) cermet anodes sintered at different temperatures, measured at 1000°C. The anodes were prepared from cermet powder coarsened at 1300°C.

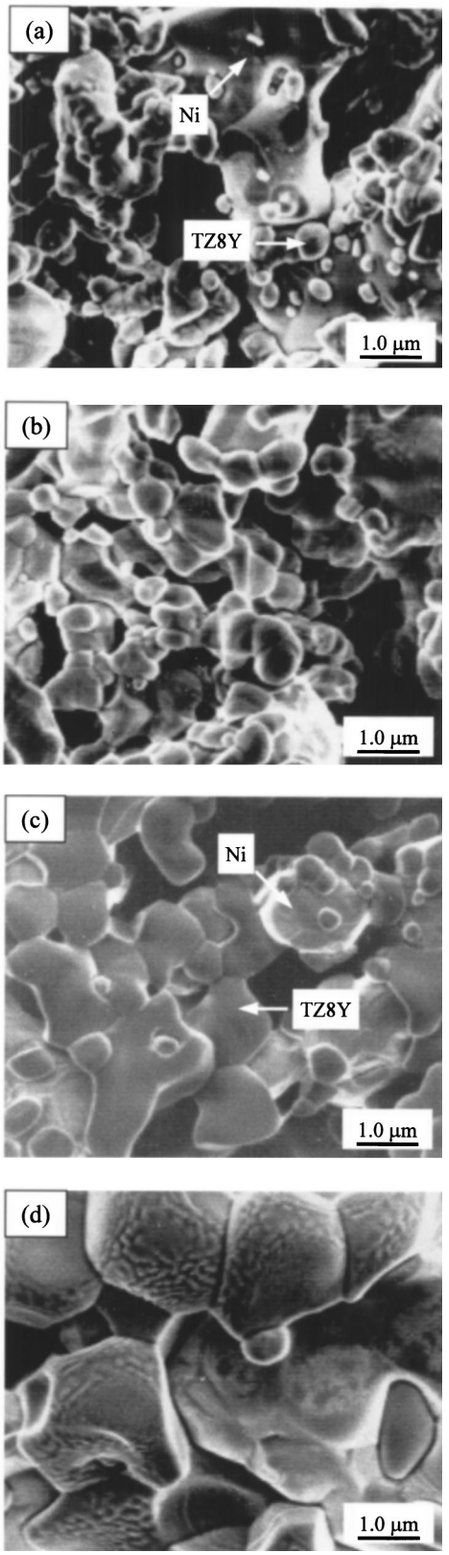

Figure 14. SEM pictures of the Ni (50 vol %)/TZ8Y (50 vol %) cermet anodes sintered at (a) 1300, (b) 1350, (c) 1400, and (d) 1500°C after fuel cell testing. The anodes were prepared from cermet powder coarsened at 1300°C.

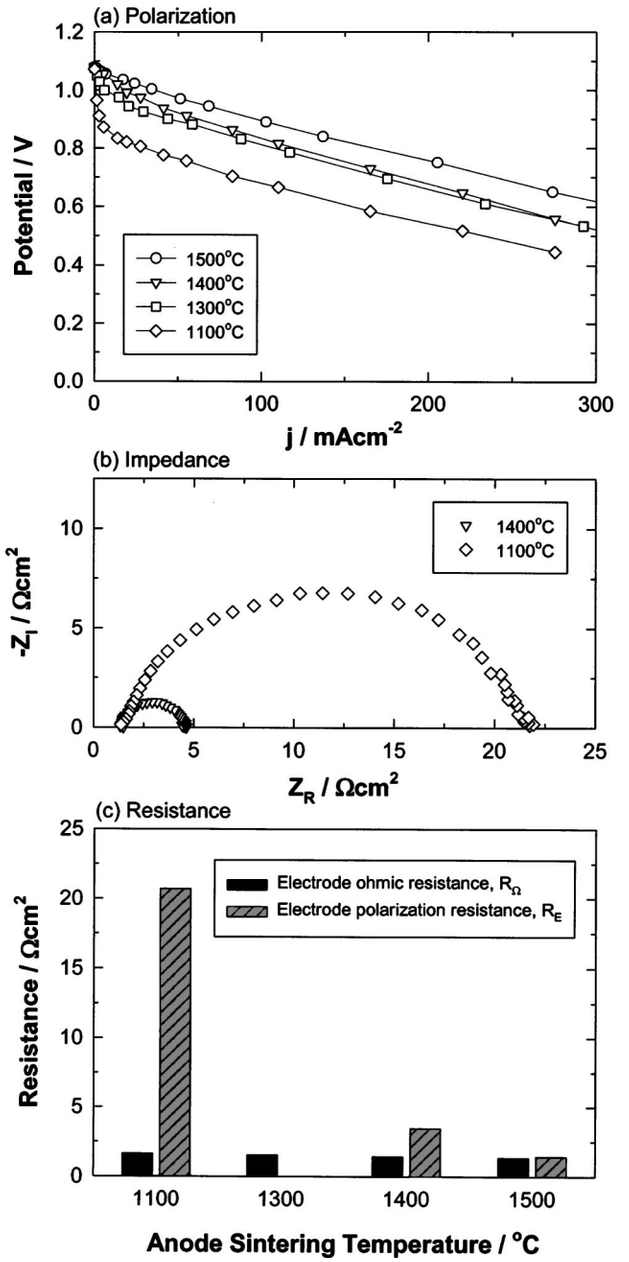

Figure 15. Effect of sintering temperature on the electrode performance of Ni anodes. (a) polarization curves, (b) impedance curves, and (c) resistance plots. Polarization and impedance curves were measured at 1000°C.

electrode and electrolyte interface region because impurities such as SiO_2 may move away or segregate from the interface region due to the increased mobility of the species at high temperatures. The formation of a good interface with fewer impurities would lead to the reduction in the electrode polarization resistance.

Discussion

The results of this comparative investigation of the fabrication and performance of Ni/TZ3Y and Ni/TZ8Y cermet anodes show the following:

1. The sintering and grain growth profiles of NiO, TZ3Y, and TZ8Y powders were significantly different in the temperature range studied. TZ3Y powders showed a generally sluggish sintering process, and the grain growth is relatively small for the powder coarsened up to 1400°C. In comparison, TZ8Y showed a very fast sintering process and rapid grain growth.

Table I. Effect of the coarsening treatment of zirconia and Ni/zirconia cermet powders and anode sintering temperature on the electrode performance of Ni/TZ3Y and Ni/TZ8Y cermet anodes.

Processing parameters	Ni/TZ3Y anode	Ni/TZ8Y anode
Zirconia coarsening temperature, T_{c1}	No significant effect; R_E increased slightly.	Significant effect; R_Ω reached minimum at T_{c1} of ~1200°C; but R_E increased substantially.
Ni/zirconia cermet coarsening temperature, T_{c2}	No significant effect; but coating quality was improved.	Significant effect; R_E and R_Ω reached minimum at T_{c2} of ~1300°C.
Anode sintering temperature, T_s	Significant effect; R_E and R_Ω reached a minimum at T_s of ~1400°C.	Significant effect; R_E and R_Ω reached minimum at T_s of ~1400°C.[a]

[a] Anode sintering temperature, T_s, is most likely related to T_{c2}, the coarsening temperature of the Ni/TZ8Y cermet powder.

2. Coarsening TZ3Y powder has no positive effect on the electrode activity of the Ni/TZ3Y cermet anodes. In fact, coarsening of TZ3Y powder at high temperatures (*e.g.*, 1400°C) increased the electrode polarization resistance and thus was detrimental to the electrode performance. The effect of the coarsening treatment of Ni/TZ3Y cermet powder on the electrode polarization performance is very small. Nevertheless, coarsening treatment improves the electrode coating quality.

3. Coarsening treatment of TZ8Y and Ni/TZ8Y cermet powders had a profound effect on the electrode performance. However, the effect of the coarsening treatment of TZ8Y and Ni/TZ8Y cermet powder differed in their effectiveness. Coarsening treatment of TZ8Y powder was mainly effective in the reduction of R_Ω. On the other hand, coarsening treatment of Ni/TZ8Y cermet powder was effective in the reduction of both R_Ω and R_E. The optimum coarsening temperature of Ni/TZ8Y cermet powder was 1300°C for the anode sintered at 1400°C.

4. A high anode sintering temperature was essential for Ni/TZ3Y and Ni/TZ8Y cermet anodes to achieve high electrode performance. R_Ω and R_E reached the lowest values for anodes sintered at 1400°C. For the pure Ni anode, R_Ω was independent of the anode sintering temperature.

Table I summarizes the effect of the coarsening treatment of zirconia and Ni/zirconia cermet powders and anode sintering temperature on the electrode performance of Ni/TZ3Y and Ni/TZ8Y cermet anodes investigated under identical conditions. The very different behavior of Ni/TZ3Y and Ni/TZ8Y cermet anode in respect to the coarsening treatment of zirconia and Ni/zirconia cermet powders can be explained based on the significant difference in the sintering behavior of TZ3Y and TZ8Y powders.

The sintering kinetics of yttria-zirconia powders varies significantly depending on the impurity content and the yttria dopant level.[20,21,28,29] For specimens prepared by isopressing and sintered at 1500°C, the average grain size of TZ8Y and TZ3Y was 5.4 and 0.56 μm, respectively.[21] High-temperature annealing treatment of TZ8Y and TZ3Y specimens at 1600°C in He or Ar increased the TZ8Y and TZ3Y grain size to ~10 and ~0.7 μm, respectively.[20] The grain size of TZ8Y is almost ten times bigger than that of the TZ3Y specimens. The difference in the sintering behavior of TZ3Y and TZ8Y appears to be more pronounced in the powder form. As shown in the present results of the particle size distribution measurement of TZ3Y and TZ8Y powders as a function of coarsening temperature, the grain growth and agglomeration of TZ8Y powders were substantial as compared to that of TZ3Y and NiO powders, despite the fact that the initial particle characteristics (particle size distribution and particle size) of TZ3Y and TZ8Y powders were very similar (see Fig. 1). Grain growth in tetragonal zirconia (*e.g.*, TZ3Y) occurs very slowly and is much more sluggish than that of cubic zirconia (*e.g.*, TZ8Y), and this has been explained by the much smaller grain boundary mobility and its high activation energy in tetragonal zirconia as compared to that in cubic zirconia.[28]

The sintering behavior and shrinkage of NiO also depend strongly on the source of the supply.[19,30] However, as shown by Matsushima *et al.*,[31] the sintering profile of the NiO/zirconia cermets is primarily dominated by that of the zirconia phase rather than that of the NiO phase. The addition of NiO reduced the activation energies of sintering of NiO/TZ8Y cermets compared to that of the TZ8Y by about 100 kJ mol^{-1}.[30,32] Upadhyaya *et al.* studied the densification behavior of 3 mol % Y_2O_3-ZrO_2 powder prepared by the co-precipitation method and found that the maximum shrinkage occurred at temperatures of 1020°C and the total shrinkage for the isopressed specimen sintered at 1400°C was ~23%.[33] For nanosized 3 mol % Y_2O_3-ZrO_2 powder, the maximum shrinkage rate occurs at ~1075°C, and the total shrinkage is ~27%.[34] This is close to the shrinkage of 26% for 8 mol % Y_2O_3-ZrO_2 powders.[31] The TZ8Y powder used in the present study had a total shrinkage of ~24%. Tietz *et al.* characterized eight different commercial NiO powders.[30] The shrinkage of the majority of the commercial NiO powders ranged from 12 to 27% and the maximum shrinkage rates occurred at temperatures between 660 to 1085°C. On the other hand, it has been reported that the maximum sintering rate for 8 mol % Y_2O_3-ZrO_2 powders and cubic zirconia powders such as Ce-doped zirconia occurs at ~1300°C.[31,35] Steil *et al.* observed an almost complete densification of YSZ at temperature around 1270°C.[36] This indicates that the shrinkage process of NiO powder would occur at temperatures close to that of 3 mol % Y_2O_3-ZrO_2 powders as compared to that of 8 mol % Y_2O_3-ZrO_2 powders. Furthermore, as suggested by Lange,[37] the maximum sintering rate corresponds to a transition from densification kinetics to coarsening (*i.e.*, grain growth) kinetics. As shown by the results of the particle size analysis as a function of powder coarsening temperature (Fig. 5), grain growth of TZ8Y powders is significantly pronounced as compared to the relatively sluggish grain growth kinetics of the TZ3Y and NiO powders. Therefore, the significant differences in the maximum shrinkage temperature and the grain growth kinetics between TZ8Y and NiO powders as compared to that between TZ3Y and NiO powders could be the fundamental reasons for the observations of the significant effect of the coarsening treatment of TZ8Y powder and/or Ni/TZ8Y cermet powders on the electrode performance of Ni/TZ8Y cermet anodes. Thus, reducing the sintering and grain growth of the TZ8Y powder in particular to the level compatible with that of the NiO phase in the cermet would be important for the formation of the continuous Ni-to-Ni connectivity in the cermet. For example, coarsening Ni/TZ8Y cermet powder at 1300°C would reduce the grain growth and shrinkage of the TZ8Y phase considerably in the cermet, thus reducing the detrimental effect of the shrinkage and grain growth on the formation of the Ni-to-Ni contact during the anode sintering process. For Ni/TZ3Y cermet anodes, the coarsening treatment of TZ3Y powder or Ni/TZ3Y cermet powder had little effect on the electrode performance of the anodes. The reason could be due to the closer maximum shrinkage temperature

and similar sluggish grain growth kinetics of both TZ3Y and NiO powders. In fact the coarsening treatment of TZ3Y increased the electrode polarization resistance and led to the increase in the polarization losses.[19]

For sintered and relatively dense Ni/YSZ cermets, the threshold of the Ni content in the cermet for the sharp increase of conductivity occurs at 30 vol % Ni.[38] This percolation behavior can be explained by the presence of the two conduction mechanisms through the cermet, an electronic path through the Ni phase and an ionic path through the YSZ phase. Above 30 vol % Ni, the conductivity is orders of magnitude higher, indicating a change in the conduction mechanism from ionic to electronic conduction.[38] For the porous Ni/YSZ cermet coating sintered on an alumina plate, the conductivity of Ni/YSZ cermet anodes was found to be dominated by the electronic conduction through the Ni phase when the Ni content was above 40 vol %.[39] However, the percolation theory of the conductivity behavior of Ni/YSZ cermet materials may not be directly applicable to the conductivity or electrode ohmic resistance behavior of the Ni/YSZ cermet electrode coating on the YSZ electrolyte as shown in this study. As electrode ohmic resistance (R_Ω) is measured between the anode and Pt reference electrode located on the opposite side of the anode. R_Ω would also depend on the electrical contact between the electrode and the YSZ electrolyte in addition to the in-plane resistance of the coating. In the case of pure Ni anode, R_Ω measured between the Ni anode and the Pt reference electrode is independent of the anode sintering temperature. This shows that the electrical contact between the pure Ni anode and the YSZ electrolyte does not depend on the anode sintering temperature as expected. However, in the case of Ni/YSZ cermet anodes, R_Ω decreases with the increase in the anode sintering temperature, indicating that the electrical contact between the Ni phase in the cermet and the YSZ electrolyte is dependent on the anode sintering temperature. Moreover, such dependence appears to be closely related to the sinterability of the YSZ phase in the cermet. As shown in Fig. 11–14, R_Ω reached a minimum for the Ni/TZ3Y and Ni/TZ8Y cermet anodes sintered at 1400°C, and at this anode sintering temperature, a continuous and rigid YSZ-to-YSZ contact network was also formed. As shown earlier,[25] the YSZ phase in the cermet bonds strongly to the YSZ electrolyte after sintering at 1400°C, forming a three-dimensional YSZ skeleton. For Ni/TZ3Y and Ni/TZ8Y cermet anodes sintered at temperatures lower than 1400°C, R_Ω increased significantly, indicating reduced electrical contact between the Ni phase in the cermet and the YSZ electrolyte. At anode sintering temperatures lower than 1400°C, the YSZ phase in the cermet did not fully sinter, and there was no formation of an intimate bonding between YSZ particles. The loosely contacted and evenly distributed fine YSZ particles would inhibit the connectivity between Ni particles and thus the formation of a continuous Ni-to-Ni network. The Ni-to-Ni network should not only be two-dimensional as required by the percolation theory but also be three-dimensional to form a good electrical contact with the YSZ electrolyte. High R_Ω values indicate poor electrical contact between the anode and YSZ electrolyte. The importance of the interface contact between Ni/YSZ cermet anode and YSZ electrolyte on the electrode ohmic resistance has also been highlighted by Koide *et al.*[39] Huebner *et al.*[10] investigated the effect of the sintering temperature of Ni/TZ8Y cermet anodes on the conductivity of the electrode coating. They observed very low conductivity ($\sim$4 S cm^{-1} at 1000°C) of the Ni/TZ8Y cermet anode sintered at 1300°C and when the anode sintering temperature increased to 1400 and 1500°C, the electronic conductivity of the same anode increased to 160 and 800 S cm^{-1}, respectively. The electrode performance of the anodes also significantly improved. Matsushima *et al.* studied the effect of sinterability of TZ8Y powder on the electrical conductivity and sintering behavior of Ni/TZ8Y cermets and found that the electrical conductivity of the cermet is dependent on the coarsening treatment of the TZ8Y powder.[31] For the cermet prepared from as-received TZ8Y powder, the conductivity was as low as 0.02 S cm^{-1} for the cermet with 40 wt % NiO content and increased to $\sim$1000 S cm^{-1} at 900°C when the NiO content increased to 60 wt %. However, the conductivity of the cermet specimen prepared from the TZ8Y powder coarsened at 1200°C was almost constant at $\sim$1000 S cm^{-1} at 900°C in the NiO content range of 40 to 60 wt %. As the high conductivity of the Ni/YSZ cermets is the result of the establishment of a continuous Ni-to-Ni electronic contact,[38] this indicates that the sintering behavior of zirconia in the cermet has a significant effect on the formation of the Ni-to-Ni electronic connectivity of the electrode coating. Sintering Ni/zirconia cermet anodes at high temperatures ($\sim$1400°C in the present study) is essential for achieving both low electrode ohmic resistance and polarization resistance for both Ni/TZ3Y and Ni/TZ8Y cermet anodes. As the sintering temperature has no effect on the electrode ohmic resistance of the pure Ni anode (Fig. 15), the significant change of the electrode ohmic resistance of Ni/zirconia cermet anodes with the sintering temperature (Fig. 11 and 13) clearly indicates that the sintering behavior (densification and grain growth) of the zirconia phase on the cermet affect not only the formation of the zirconia-to-zirconia ionic network, but also the formation of the Ni-to-Ni electronic network. The formation of a continuous Ni-to-Ni electronic network essentially reduces the in-plane resistance of the anode and improves the electrical contact between the Ni phase in the cermet and YSZ electrolyte, indicated by the decrease of the electrode ohmic resistance. The formation of a rigid YSZ-toYSZ networking for the cermet anodes sintered at 1400°C stabilizes the Ni/YSZ cermet structure and substantially increased the electrochemical reaction areas by extension of the three-phase boundary into the cermets, thus reducing the electrode polarization resistance significantly.[25] It appears that the formation of YSZ-to-YSZ ionic network and Ni-to-Ni electronic network occurs almost at the same time at temperatures around 1400°C, as indicated by the simultaneous decrease of both R_Ω and R_E. The development of the ionic and electronic network provides the continuous electronic and ionic path and is critical for the high performance SOFC anodes, as shown by the anode micromodel developed by Chan and Xia.[40] The simultaneous reduction of the R_Ω and R_E was also observed by Primdahl *et al.* on Ni/YSZ anodes sintered at temperatures of 1300 to 1400°C.[12]

Finally, the selection of Ni/TZ3Y and Ni/TZ8Y cermet compositions in this study is somewhat arbitrary due to the early stages of the development of the Ni/zirconia cermet anodes. However, similar effects of coarsening treatment of TZ3Y and Ni/TZ3Y cermet powder and anode sintering temperature have also been observed on the performance of Ni (50 vol %)/TZ3Y (50 vol %) cermet anodes prepared by screenprinting methods.[19] This indicates that the direct comparison of the effect of sintering behavior of the zirconia phase in the cermet on the fabrication and performance of Ni (70 vol %)/TZ3Y (30 vol %) and Ni (50 vol %)/TZ8Y (50 vol %) cermet anodes studied here would still be valid despite the difference in the Ni content. Thus, the results from the present investigation should have general implications for the development of Ni/zirconia cermet anodes for SOFCs.

Conclusions

The fabrication processes, such as the effect of coarsening temperature of zirconia and Ni/zirconia cermet powders and sintering temperatures of cermet anodes, were investigated on Ni/TZ3Y and Ni/TZ8Y cermet electrodes. Fabrication processes of Ni/zirconia cermet anodes are critically dependent on the sintering properties of the zirconia phase. The results indicate that the sintering behavior and properties of the zirconia phase on the cermet affect not only the formation of the zirconia-to-zirconia ionic network but also the formation of Ni-to-Ni electronic network. The results demonstrated that the fabrication process, microstructure, and electrode performance are strongly affected by the sintering behavior of the zirconia phase in the cermets.

Acknowledgments

I thank Kylie Crane for technical assistance in the preparation of cermet anodes and electrolyte substrates and Dr. John Drennan and Shirley Green for TEM and SEM analysis.

References

1. N. Q. Minh, *J. Am. Ceram. Soc.*, **76**, 563 (1993).
2. J. P. P. Huijsmans, *Curr. Opin. Solid State Mater. Sci.*, **5**, 317 (2001).
3. S. P. Jiang and Y. Ramprakash, *Solid State Ionics*, **116**, 145 (1999).
4. E. Ivers-Tiffée, W. Wersing, M. Shießl, and H. Greiner, *Ber. Bunsenges. Phys. Chem.*, **94**, 978 (1990).
5. R. Vasen, D. Simwonis, and D. Stover, *J. Mater. Sci.*, **36**, 147 (2001).
6. S. P. Jiang and S. P. S. Badwal, *Solid State Ionics*, **123**, 209 (1999).
7. T. Kawada, N. Sakai, H. Yokokawa, and M. Dokiya, *J. Electrochem. Soc.*, **137**, 3042 (1990).
8. B. de Boer, M. Gonzalez, H. J. M. Bouwmeester, and H. Verweij, *Solid State Ionics*, **127**, 269 (2000).
9. M. Brown, S. Primdahl, and M. Mogensen, *J. Electrochem. Soc.*, **147**, 475 (2000).
10. W. Huebner, D. M. Reed, and H. U. Anderson, in *Solid Oxide Fuel Cells-VI* S. C. Singhal and M. Dokiya, Editors, PV 99-19, p. 503, The Electrochemical Society Proceeding Series, Pennington, NJ (1999).
11. E. Z. Tan, T. H. Etsell, and D. G. Ivey, *J. Am. Ceram. Soc.*, **83**, 1626 (2000).
12. S. Primdahl, B. F. Sørensen, and M. Mogensen, *J. Am. Ceram. Soc.*, **83**, 489 (2000).
13. T. Setoguchi, K. Okamoto, K. Eguchi, and H. Arai, *J. Electrochem. Soc.*, **139**, 2875 (1992).
14. S. P. Jiang and S. P. S. Badwal, *J. Electrochem. Soc.*, **144**, 3777 (1997).
15. A. Ringuedé, D. Bronine, and J. R. Frade, *Solid State Ionics*, **146**, 219 (2002).
16. S. P. Jiang, Y. Y. Duan, and J. G. Love, *J. Electrochem. Soc.*, **149**, A1175 (2002).
17. F. P. F. van Berkel, F. H. van Heuveln, and J. P. P. Huijsmana, in *Solid Oxide Fuel Cells-III*, S. C. Singhal and H. Iwahara, Editors, PV 93-4, p. 744, The Electrochemical Society Proceeding Series, Pennington, NJ (1993).
18. H. Itoh, T. Yamamoto, M. Mori, T. Horita, N. Sakai, H. Yokokawa, and M. Dokiya, *J. Electrochem. Soc.*, **144**, 641 (1997).
19. S. P. Jiang, P. J. Callus, and S. P. S. Badwal, *Solid State Ionics*, **132**, 1 (2000).
20. R. A. Cutler, J. R. Reynolds, and A. Jones, *J. Am. Ceram. Soc.*, **75**, 2173 (1992).
21. F. T. Ciacchi, K. M. Crane, and S. P. S. Badwal, *Solid State Ionics*, **73**, 49 (1994).
22. T. Sato and M. Shimada, *J. Am. Ceram. Soc.*, **68**, 356 (1985).
23. X. Guo, *J. Mater. Sci.*, **36**, 3737 (2001).
24. J. van Herle, R. Ihringer, and A. J. McEvoy, in *Solid Oxide Fuel Cell V*, U. Stimming, S. C. Singhal, H. Tagawa, and W. Lehnert, Editors, PV 97-40, p. 565, The Electrochemical Society Proceeding Series, Pennington, NJ (1997).
25. S. P. Jiang, *J. Electrochem. Soc.*, **148**, A887 (2001).
26. K. V. Jensen, S. Primdahl, I. Chorkendorff, and M. Mogensen, *Solid State Ionics*, **144**, 197 (2001).
27. M. Mogensen, K. V. Jensen, M. J. Jørgensen, and S. Primdahl, *Solid State Ionics*, **150**, 123 (2002).
28. I. G. Lee and I-W. Chen, in *Sintering '87*, S. Sōmiya, M. Shimada, M. Yoshimura, and R. Watanabe, Editors, p. 340, Elsevier Applied Science, London (1988).
29. J. Zhao, Y. Ikuhara, and T. Sakuma, *J. Am. Ceram. Soc.*, **81**, 2087 (1998).
30. F. Tietz, F. J. Dias, D. Simwonis, and D. Stöver, *J. Euro. Ceram. Soc.*, **20**, 1023 (2000).
31. T. Matsushima, H. Ohrui, and T. Hirai, *Solid State Ionics*, **111**, 315 (1998).
32. I. R. Gibson, D. P. Dransfield, and J. T. S. Irvine, *J. Mater. Sci.*, **33**, 4297 (1998).
33. D. D. Upadhyaya, T. R. G. Kutty, and C. Ganguly, in *Science and Technology of Zirconia V*, S. P. S. Badwal, M. J. Bannister, and R. H. J. Hannink, Editors, p. 310, Technomic Publishing Co., Lancaster, PA (1993).
34. S. K. Tadokoro and E. N. S. Muccillo, *J. Alloys Compd.*, **344**, 186 (2002).
35. I. M. G. dos Santos, R. C. M. Moreira, E. R. Leite, E. Longo, and J. A. Varela, *Ceram. Int.*, **27**, 283 (2001).
36. M. C. Steil, F. Thevenot, and M. Kleitz, *J. Electrochem. Soc.*, **144**, 390 (1997).
37. F. F. Lange, *J. Am. Ceram. Soc.*, **72**, 3 (1989).
38. D. W. Dee, T. D. Clarr, T. E. Easler, D. C. Fee, and F. C. Mrazek, *J. Electrochem. Soc.*, **134**, 2141 (1987).
39. H. Koide, Y. Someya, T. Yoshida, and T. Maruyama, *Solid State Ionics*, **132**, 253 (2000).
40. S. H. Chan and Z. T. Xia, *J. Electrochem. Soc.*, **148**, A388 (2001).